

Experimental Evaluation of PWM Control Technique for an NPC Inverter to feed an Asynchronous Machine Using DSP Controller

H. DENOUN, N. BENYAHIA, M. ZAOUIA, N. BENAMROUCHE, S. HADDAD, S. AIT MAMAR

Abstract— This paper discusses modelling and control of an a neutral point clamped (NPC) inverter called three-level inverter witch operates with the PWM switching pattern using DSP.

The mathematical model of the (NPC) inverter is carried out using the conversion and connection functions for an easier understanding of the system operation. Simulation results using *matlab* program are reported in this paper.

The performance obtained for the drivers of an asynchronous machine fed by this inverter are interesting. Finally, an analysis and experimental results validate the effectiveness of the proposed control solution.

Key words— Pulse Width Modulation (PWM), Total harmonic distortion (THD), Neutral Point Clamping (NPC), Multilevel Inverter, Digital Signal Processor (DSP), IGBT, Matlab simulink, Machine asynchronous.

I. INTRODUCTION

UP to now, many studies have been presented on multilevel inverters including many topologies, but the (NPC) inverter topology is famous one and attracting many researchers over the world.

The three-level inverter (NPC) shown in fig.1 has been introduced to enhance the handling capacity of power electronics using currently switching devices without any problematic connections like transformer or series connections [1]. This topology of inverter is suitable for high voltage and high power inversion because the forward blocking voltage capability for giving devices is double and also due to its ability to synthesize wave forms with better harmonic spectrum and low switching frequency [2].

In this paper, the mathematical model of the NPC inverter is done using the conversion and connection function for an easier understanding of the system operation according to the possible combination of switching states of the switching device on one leg.

The control technique applied to the NPC inverter is studied. This paper present also in detail the control systems of the inverter in order to produce inverter output for application using *Texas Instruments* Microcontroller (DSP).

This work was supported in part by LATAGE research laboratory, University Mouloud Mammeri, of Tizi-Ouzou, 15000 Algeria.

Hakim Denoun is with the Electrical and Computer Engineering department at Mouloud Mammeri University of Tizi-Ouzou, Algeria, P.O. Box 17, Tizi-Ouzou, Algeria, [Tel:+213555185198](tel:+213555185198); email : akim_danoun2002dz@yahoo.fr. Nacereddine Benamrouche is with the Electrical and Computer Engineering department at Mouloud Mammeri University of Tizi-Ouzou, Algeria University, P.O. Box 17, Tizi-Ouzou, Algeria, (tel : +213772314992; email : benamrouchen@yahoo.fr).

DSP is new generation of controller with a main frequency of 150MHz. The speed and the features of this DSP make it in excellent choice for the digital control of an inverter.

Experimental results obtained from NPC inverter and to feed an asynchronous machine will be presented.

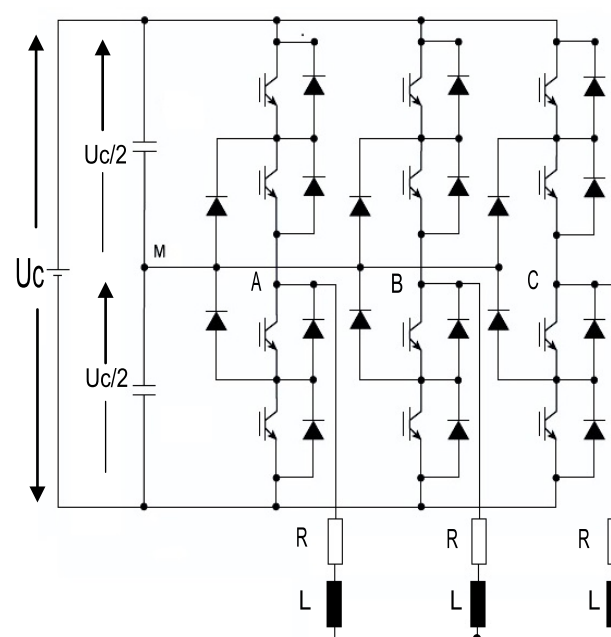


Fig.1. Power circuit of NPC inverter

The NPC multilevel inverter uses capacitors in series to divide up the DC bus voltage into different voltage levels. To produce m-levels in the phase voltage, an m-level NPC inverter needs m-1 capacitors on the dc bus. A three-phase three-level NPC inverter is shown in fig.1. The dc bus consists of two capacitors C. For a dc bus voltage U_c , the voltage across each capacitor is $U_c/2$ and each device voltage stress will be limited to one capacitor voltage level $U_c/2$ through clamping diodes [3],[4].

II. CONTROL MODEL OF A THREE-LEVEL INVERTER

A. Different configurations of the inverter

To describe the different sequences of the inverter function, let us consider the possible states of the first leg switches fig.2.

The three-level inverter has the advantages that the blocking voltage of each switching device is one half of dc-link voltage whereas full dc-link voltage for two-level inverter.

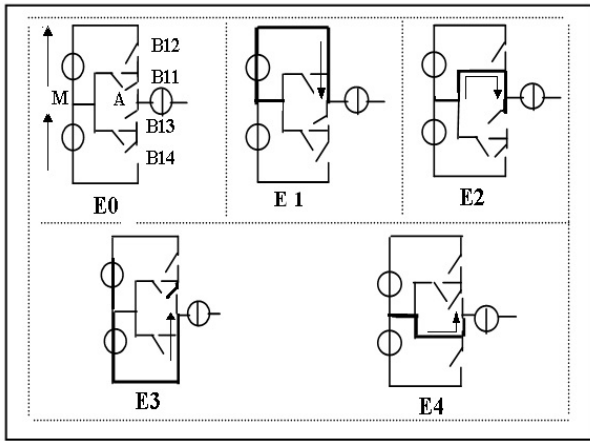


Fig.2. Different configurations of a leg

B. Complementary command

We define the complementary control of the inverter leg as follows [5] :

$$\begin{cases} B_{K1} = \bar{B}_{K4} \\ B_{K2} = \bar{B}_{K3} \end{cases} \quad (1)$$

It was demonstrated [5] that the command given by relationship (1) is the one which gives the three levels U_c , 0, $-U_c$, in a optimum way.

Table 1 shows the state of the switches and the corresponding output voltage of the inverter. Where V_k ($k = a, b, c$) is the potential of the leg.

Table I: Switches states and corresponding voltage

B_{k1}	B_{k2}	B_{k3}	B_{k4}	V_k
0	0	1	1	$-U_{c2}$
0	1	0	1	Unknown
1	0	1	0	0
1	1	0	0	U_{c1}

C. Model control of the three-level inverter - Connection functions

It defines the state of the switch. it equals 1 if the switch is ON and 0 if the switch is OFF. The connection functions of the three-level inverter are related by the following relation.

$$\begin{aligned} F_{k1} &= 1 - F_{k4} \\ F_{k2} &= 1 - F_{k3} \end{aligned} \quad (k = 1, 2, 3) \quad (2)$$

Therefore, the branch voltages V_{AM} , V_{BM} , V_{CM} are expressed as follow :

$$\begin{aligned} V_{AM} &= F_{11} \cdot F_{12} \cdot U_{C1} - F_{13} \cdot F_{14} \cdot U_{C2} \\ V_{BM} &= F_{21} \cdot F_{22} \cdot U_{C1} - F_{23} \cdot F_{24} \cdot U_{C2} \\ V_{CM} &= F_{31} \cdot F_{32} \cdot U_{C1} - F_{33} \cdot F_{34} \cdot U_{C2} \end{aligned} \quad (3)$$

However, the output phase voltage of the inverter can be deduced from the relation (3) as follow:

$$\begin{aligned} V_A &= (2V_{AM} - V_{BM} - V_{CM}) / 3 \\ V_B &= (2V_{BM} - V_{CM} - V_{AM}) / 3 \\ V_C &= (2V_{CM} - V_{AM} - V_{BM}) / 3 \end{aligned} \quad (4)$$

And these equations can be rewritten using the voltage branches which give :

$$\begin{bmatrix} V_A \\ V_B \\ V_C \end{bmatrix} = \frac{1}{3} \begin{bmatrix} 2 & -1 & -1 \\ -1 & 2 & -1 \\ -1 & -1 & 2 \end{bmatrix} \begin{Bmatrix} F_{11}F_{12} \\ F_{21}F_{22} \\ F_{31}F_{32} \end{Bmatrix} U_{C1} - \begin{bmatrix} F_{13}F_{14} \\ F_{23}F_{24} \\ F_{33}F_{34} \end{bmatrix} U_{C2} \quad (5)$$

In most applications, AC machines are preferable to DC machines due to their easy and more robust construction without any mechanical switch. DC motors have been used in the high-performance domain, with requires fast and precise torque control. However, due to the advancement in micro-and power electronics, high-performance control of ac motors can now be implemented at a reasonable cost.

The vector control concept has become a standard tool for high-performance control us ac motors. The ultimate objective of vector control is to enable decoupling control of torque and flux similar to the control of a separately excited dc motor.

In the case of squirrel cage induction motor drive systems, the direct and indirect methods of vector control have been applied. The direct method requires the difficult task of flux acquisition for field orientation.

The indirect method is basically a free forward slip frequency control scheme that does not require flux acquisition. Both methods provide decoupling control of torque and flux. However, the indirect method is gaining popularity due to simplicity of implementation and which is applied in this paper.

III. PWM STRATEGY AND SIMULATION RESULTS

The parameters of PWM control technique are defined as: Amplitude modulation index m_a and the frequency ratio m_f .

$$m_a = A_m / A_c \quad (6)$$

$$m_f = f_c / f_m \quad (7)$$

Where A_m is the peak amplitude of the control signal, while A_c is the peak amplitude of triangle signal (carrier). m_f is the ratio between the carrier and the control frequency.

The one carrier PWM three level inverter algorithms is :

$$\begin{aligned} (|V_{ref.1}| \leq U_p) &\Rightarrow B_{11} = 1, B_{12} = 0 \\ (|V_{ref.1}| > U_p) \text{ et } V_{ref.1} < 0 &\Rightarrow B_{11} = B_{12} = 0 \\ (|V_{ref.1}| > U_p) \text{ et } V_{ref.1} > 0 &\Rightarrow B_{11} = B_{12} = 1 \end{aligned} \quad (8)$$

Where: V_{ref} is called modulating signal

U_p is the carrier signal

Table II: shows the truth table of the algorithm [5].

A	B	B11	B12
0	0	1	0
0	1	0	0
1	1	1	1
1	0	1	0

Where:

$$A = 1 \text{ when } V_{ref} > 0 \quad \text{if not } A = 0$$

$$B = 1 \text{ when } |V_{ref}| > U_p \quad \text{if not } B = 0$$

The logical expressions of B₁₁ and B₁₂ are:

$$B_{11} = \overline{B_{14}} = \overline{B} + A$$

$$B_{12} = \overline{B_{13}} = AB \tag{9}$$

The synoptic diagram of the proposed simulation of the strategy is shown in fig. 3 [6], [7].

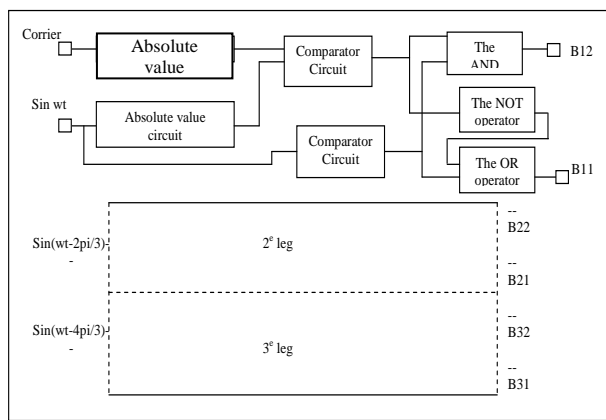


Fig.3 Synoptic of the proposed PWM strategy

To illustrate the performance of the three-level PWM inverter, the systems was investigated through computer simulation under no load. Fig.4, shows the phase voltage at $m_f=24$ and $m_a=0.8$ with a sinusoidal triangle PWM and contains harmonics greater which can be easily filtered and the results are much better than conventional two-level inverter. The comparison of the reference sinusoidal signal with the triangular waveform is done in the PWM generator of the DSP to generate the control signals for the switching devices along with the inverted signals with the required dead band.

By taking the following parameters:
 $R=22\ \Omega$, $L=340\text{mH}$, $m_f=24$, $m_a=0.8$. $U_c/2=30\text{V}$,
 $f=50\text{Hz}$.

The obtained simulation results are illustrated by fig.4, 5, 6, 7, 8.

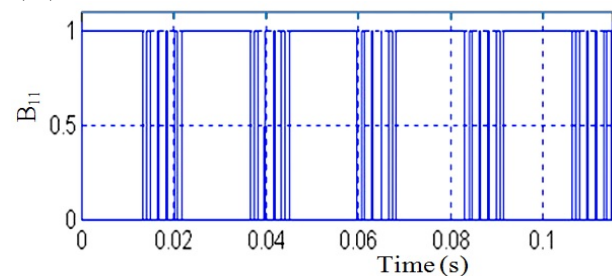


Fig.4 Control pulses for $m_f=24$ $m_a=0.8$

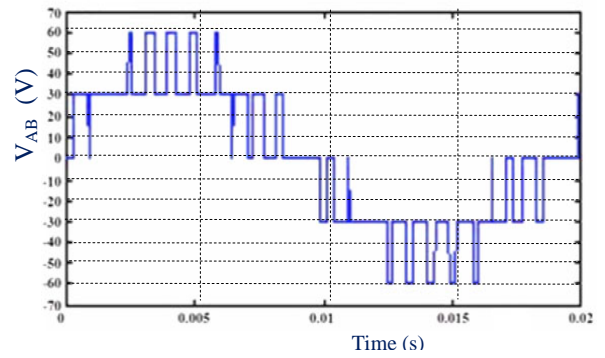


Fig.5. Voltage V_{AB}

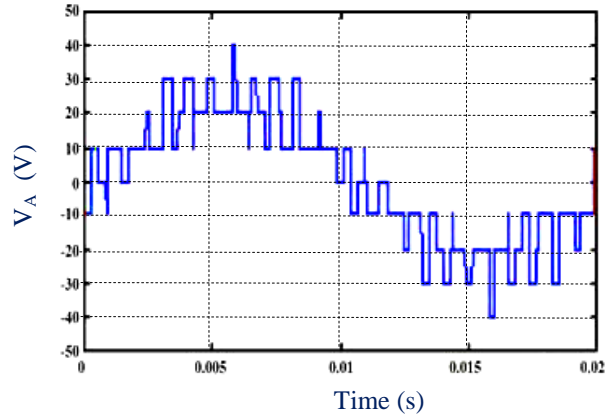


Fig.6 Output voltage of phase V_A

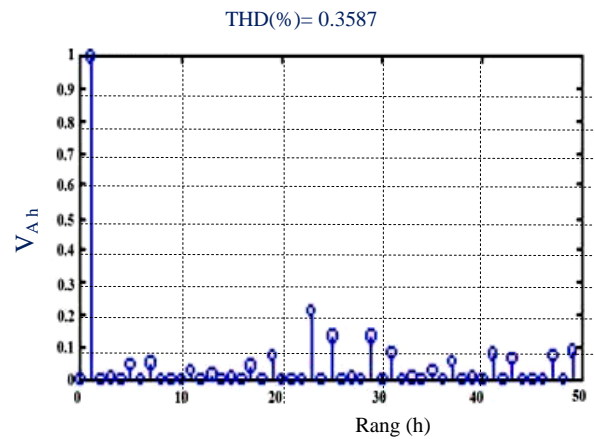


Fig.7

V_A harmonic spectrum and THD

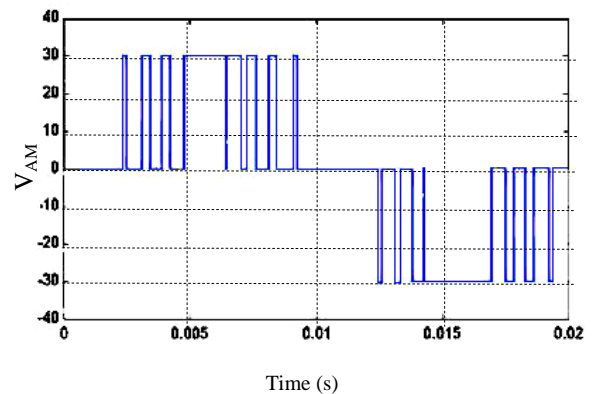


Fig.8 Voltage V_{AM}

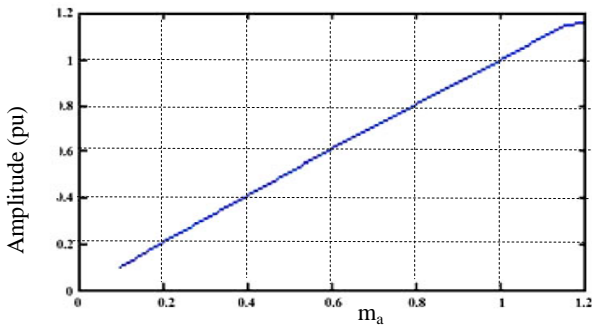


Fig.9 Evolution of the fundamental voltage V_A .

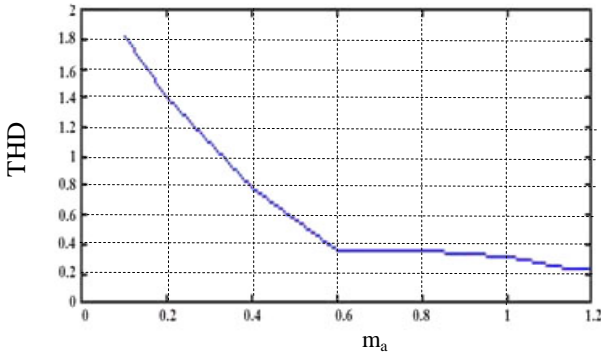


Fig.10 THD of voltage V_A

Fig.4 shows the simulation sequences of upper-arm.
 Fig.5 shows the line voltage V_{ab} . It has five voltage levels $2U_c / 2, U_c / 2, 0, -U_c / 2, 2U_c / 2$.
 Fig.6 shows the output voltage of the first phase of the inverter.
 Fig.7 shows the V_a analysis spectral. The voltage spectrum shows that the harmonics are grouped into multiple frequencies centered around the frequency switching families. the most important harmonics are numbered number 23 and 25.
 Fig.8 shows the voltage V_{AM} . It shows three levels of output voltage of an arm $U_c/2, 0, -U_c/2$.
 Fig.9 shows the evolution of the amplitude of the fundamental output voltage V_A versus the rate setting m_a .
 Fig.10 shows the curve of the harmonic versus content in terms of m_a . We note that the harmonics decreases as m_a increases.

IV. ASYNCHRONOUS MACHINE MODEL AND SIMULATION RESULTS

A. Electrical equations

The equations of induction machines are defined by the state equation as follow:

$$\frac{dX}{dt} = AX + BU$$

$$\text{where } X = \begin{bmatrix} i_{sd} \\ i_{sq} \\ i_{rd} \\ i_{rq} \end{bmatrix}; \quad U = \begin{bmatrix} V_{sd} \\ V_{sq} \end{bmatrix} \quad (10)$$

$$A = \begin{bmatrix} -R_s & 1-\sigma & M & M \\ \sigma L_s & \sigma \omega_r & \sigma L_s T & \sigma L_s \omega_r \\ 1-\sigma & -R_s & M & M \\ \sigma & \sigma L_s & -\sigma L_s \omega_r & \sigma L_s T_r \\ MR_s & -M \omega_r & 1 & \omega_r \\ \sigma L_s L_r & \sigma L_s \omega_r & \sigma T_r & \sigma \\ M & MR_s & \omega_r & 1 \\ \sigma L_r & \sigma L_s L_r & \sigma & \sigma T_r \end{bmatrix} \quad (11)$$

$$B = \begin{bmatrix} 1 & 0 \\ \sigma L_s & -1 \\ 0 & \sigma L_s \\ -M & 0 \\ \sigma L_s L_r & 0 \\ 0 & -M \\ & \sigma L_s L_r \end{bmatrix} \quad (12)$$

B. Mechanical equations

$$\begin{aligned} C_e &= 3/2 P_p M (i_{rd} i_{sq} - i_{sq} i_{rd}) \\ &= 3/2 P_p \frac{M}{L_r} (\phi_{rd} i_{sq} - i_{sd} \phi_{rq}) \end{aligned} \quad (13)$$

$$J = \frac{d\omega_m}{dt} + f \omega_m = C_e - C_r \quad (14)$$

C. Decoupling control by compensation

Fig.11 shows the block diagram of a decoupling control which is governed by the equations (15) and fig.12 is the block diagram of the indirect field oriented induction motor drive system. The power supply is characterised by a PWM voltage source inverter. The motor is controlled according to the principal of the orientation of the rotor flux which is aligned along the d-axis.

$$\begin{pmatrix} \phi_{dr} = \phi_r \\ \phi_{qr} = 0 \end{pmatrix}$$

$$V_{sd} = V_{sld} - f e m_d$$

$$V_{sq} = V_{slq} - f e m_q$$

With :

$$\begin{aligned} V_{sld} &= \frac{(\sigma L_s L_r^2) p + R_s L_r^2 + R_r M^2}{L_r^2} i_{sd} \\ V_{slq} &= \frac{(\sigma L_s L_r^2) p + R_s L_r^2 + R_r M^2}{L_r^2} i_{sq} \end{aligned} \quad (15)$$

$$Fem_d = \omega_s \sigma L_s i_{sq} + \frac{MR_r}{L_r^2} \phi_r$$

$$Fem_q = -\omega_s \sigma L_s i_{sd} - \frac{M}{L_r} \omega_s \phi_r + \frac{M^2}{L^2 T_r} i_{sq}$$

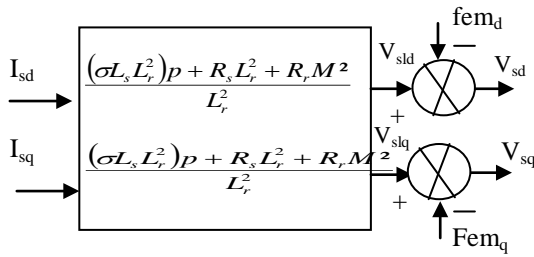


Fig.11 Decoupling control

$$i_{sd} = \frac{\phi_r (T_r p + 1)}{M}$$

$$i_{sq} = \frac{2}{3} \frac{C_e L_r}{P p M \phi_r}$$

$$\omega_{sl} = \frac{M}{\phi_r T_r} i_{sq}$$

and $\omega_s = \omega_r + \omega_{sl}$

To illustrate the performance of the three-level PWM inverter, the systems was investigated through computer simulation under no load. Fig.11 shows the phase voltage at $m_f=21$ and $m_a=0.9$ with a sinusoidal triangle PWM and contains harmonics greater which can be easily filtered and the results are much better than conventional two – level inverter. Fig.12 shows the speed variation at no load.

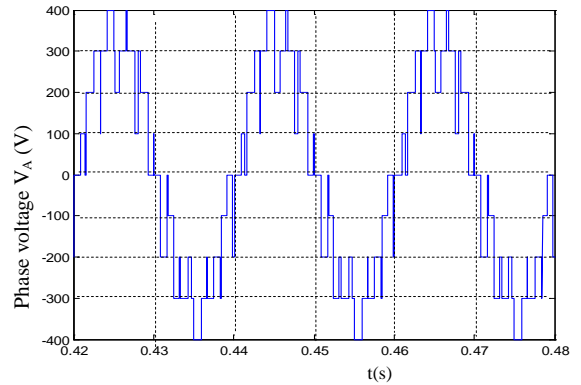


Fig.13 phase voltage (V_A)

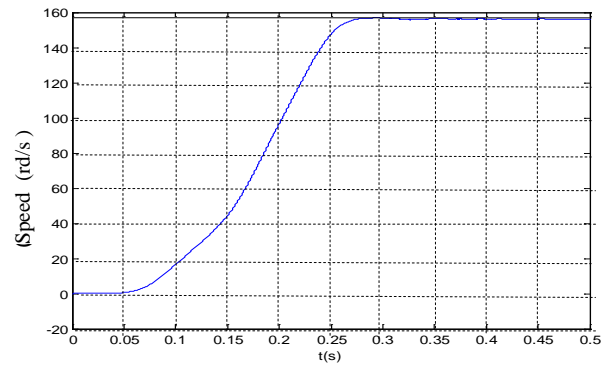


Fig. 14 speed at no load

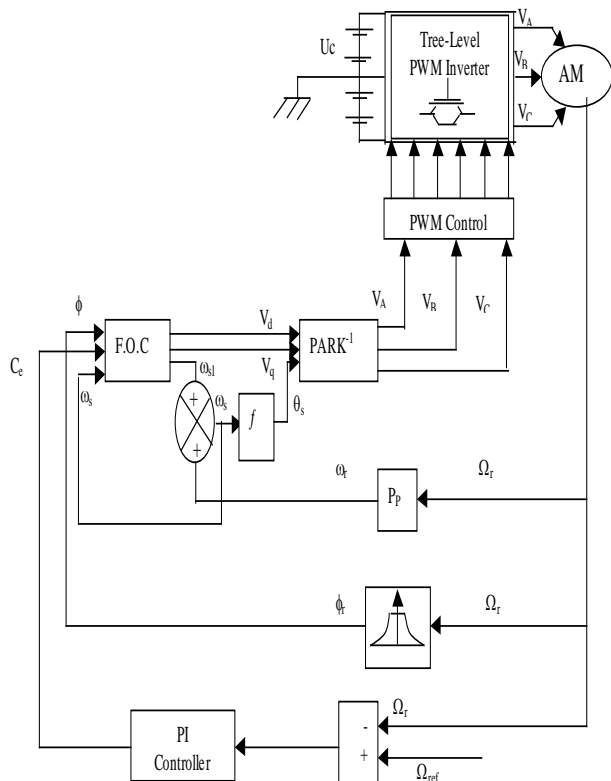


Fig.12 Block diagram of the indirect field oriented induction motor drive system fed by three – level PWM inverter with PI controller.

V. EXPERIMENTAL TESTS OF THE NPC INVERTER

The schematic diagram of the converter circuit implemented is given in fig.15. It has two parts, the control circuit and the power circuit. The shaded part is the control circuit containing the DSP controller TMS320LF2407 that generates the PWM signals and also provides soft start function [8].

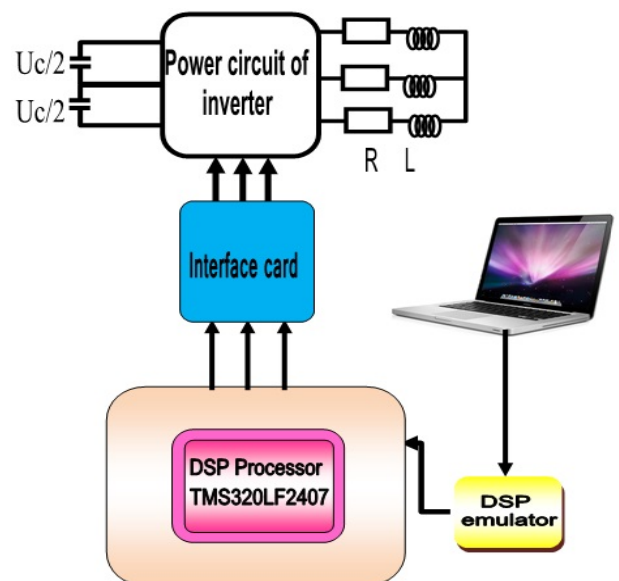


Fig.15.a DSP TMS320LF2407 implementation diagram

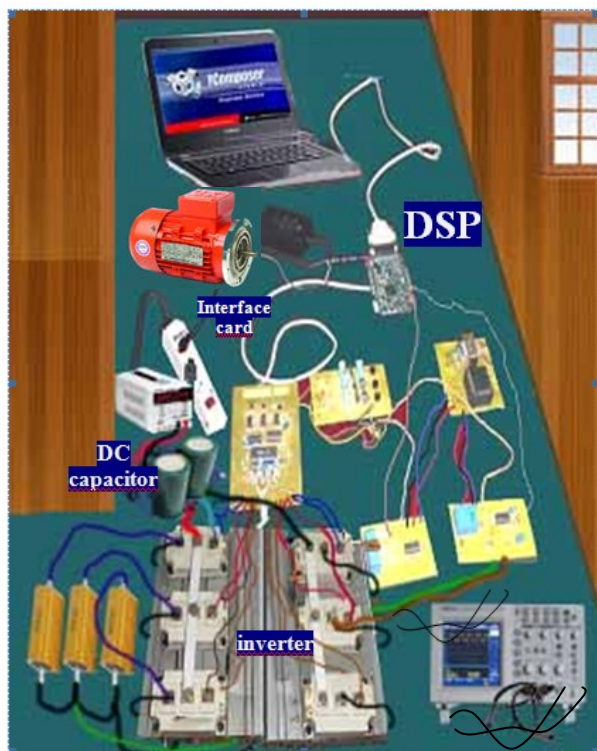


Fig.15.b Experimental bench

Later on, the three-level inverter was implemented using DSP TMS320LF2407 and its performance was studied. A comparison is made of the results obtained through simulation and experimental work under the same operating conditions. To verify the theoretical results obtained on the three-level inverter, we designed and built the various circuits forming the full inverter.

A power circuit formed by two arms, formed by twelve transistors I.G.B.T and eighteen diodes connected in anti-parallel. The generated control signals were obtained using several control cards such as conditioning, monitoring, D/A conversion cards.

Fig.15 Shows the D.S.P. TMS320LF2407 implementation diagram and experimental bench.

The DSP programming was based on the software developed by Texas Instruments "Code composer".

The control algorithm has been written in assembly language in order to optimize the whole tasks of operation and communication between the DSP, the converter and the Load [10] [11] [12] [13].

After the construction of the various circuits, the three-level inverter was tested in the laboratory; it functioned as an inverter supplying a passive load formed by a resistance and an inductance. The oscillographic results obtained are given in fig.16, 17, 18, 19.

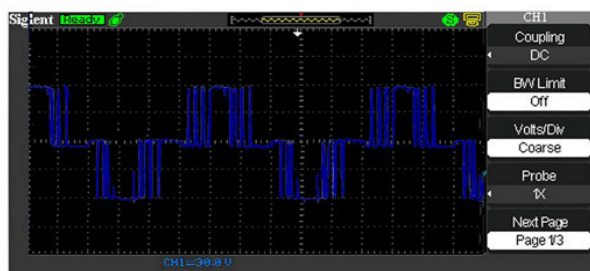
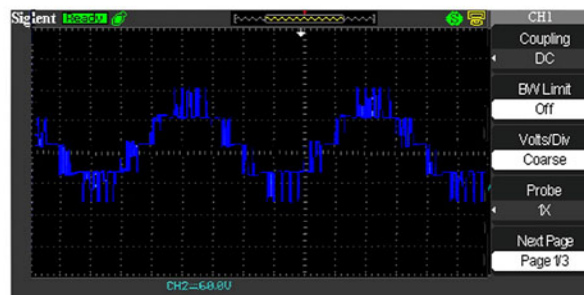
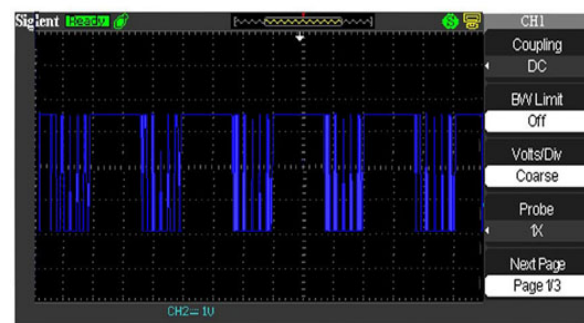
Fig.16 V_{AM} voltage (15V/Div)Fig.17 Output voltage of phase V_A (15V/Div)Fig.18 Voltage V_{AB} (30V/Div)

Fig.19 Control pulses (1v/Div)

For a triangulo-sinusoidal strategy, a cyclic ratio equal to 0.8 and the index of modulation equals 24 were taken.

Fig.16 clearly shows the V_{AM} voltage variation. The waveform of the voltage is similar to that obtained from the simulation, the difference in the zero level of the voltage that is a little shifted. This is due to the imbalance of the midpoint.

Fig.17 shows the change in the voltage of the first phase V_A . Both V_A voltage obtained in Pc simulation and experiments almost the same.

The V_{AB} Voltage was presented in fig.18.

Experimental control pulses were shown in fig.19.

Both voltages (V_{AM} , V_A , V_{AB} , B_{11}) of three level inverter obtained in pc simulation and experiments almost the same.

VI. SIMULATION AND EXPERIMENTAL RESULTS OF AN ASYNCHRONOUS MACHINE FEED PWM

The block diagram of inverter feeding asynchronous machine is represented in fig.20.

For the verification and test of PWM modulation circuits fed asynchronous machine described above, a reduced power model has been realised in research lab BT's. From INTERNATIONAL RECTIFIER (IRGBC40F), power diode from THOMSON (BYT30PI 1000) were used. The load is a three-phase

1KW asynchronous machine with rated parameters given below:
 ΔY 220/380 V 4, 7A /2,7 A
 2830 Tr / min , 50 Hz.

The no-load test of asynchronous machine measures the rotational losses of the motor and provides information.

The Inverter carrier sequence 830 Hz , $I_a = 2A$, $U_{ab} = 50V$.

The algorithms are implemented more easily by numerical circuits. The proposed control circuits are shown along with the power circuit. The PWM is proposed to control this inverter [10], [11].

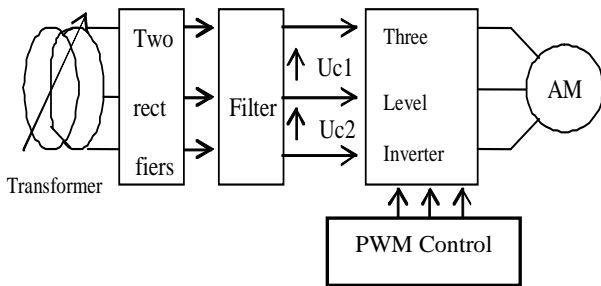
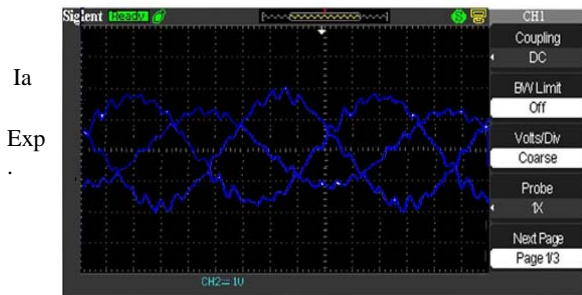
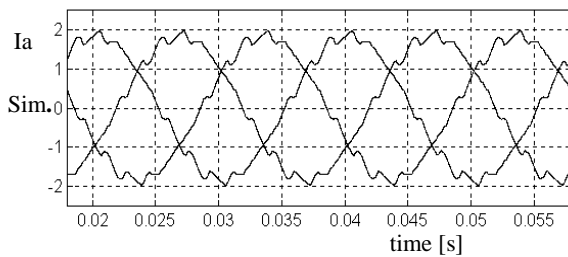


Fig.20 Block diagram A.M fed PWM



1A/Div
 Fig.21 Load current

The graphs presented in Fig.21 and Fig.22 are showing simulation and experimental line current and phase voltage. The line current generated by three-level inverter has low harmonic components even though the Switching frequency of the active devices is very low.

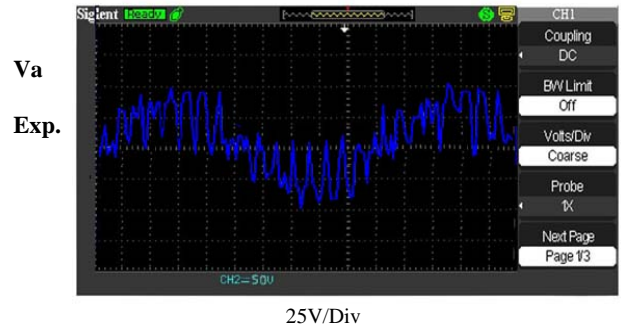
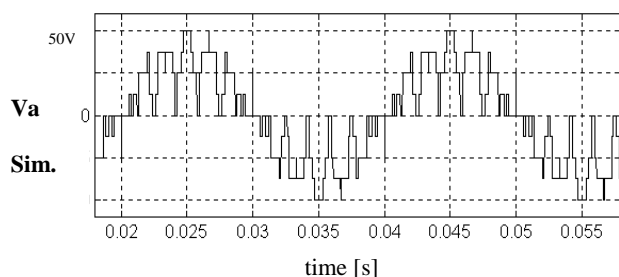


Fig.22 Load voltage

VII. CONCLUSION

This paper presents the analysis and design of a digitally controlled inverter (NPC) and asynchronous machine fed by this inverter based on DSP control application. DSP TMS320lf2407 is programmed to produce gate pulses by comparing a triangular carrier wave in high frequency and a sinusoidal reference wave in 50 Hz.

Simulation and experimental results show the feasibility of such a system. The low commutation frequency of three-level inverters permits a realisation of an optimal control by relatively simple tools. With a high number of semiconductor devices, current quality is improved and weight reduced by avoiding heavy current filters.

The control voltage was controlled by microcomputer in a much more sophisticated manner than that described here. This work opens new ways for future research because the inverter can be controlled by numerical signal. The obtained results are satisfactory because the output harmonic components phase are fewer than those obtained in conventional two-level inverters at the same switching frequency. Experimental results using the DSP confirm those obtained in numerical simulation.

APPENDIX

MACHINE PARAMETERS

Rated current	6.4A/3.7A+
Rated voltage	220/380V
Rated Power	1.5Kw
RatedSpeed	1420 rev/mn
R_s	4.85 Ω
R_r	3.805 Ω
L_s, L_r	0.274 Ω
M	0258 Ω
J	0.031
F	0.00114
P_p	2

PI Controller parameters

P	0.35
I	1.1

NOMENCLATURE

s, r	suffixes denoting stator and rotor, respectively
d, q	suffixes denoting axes rotating synchronously with the rotor
p	differential operator, d / dt
L_s, L_r	apparent self inductance per phase of stator and rotor
M	apparent mutual inductance
σ	leakage factor $(L_s L_r - M^2) / L_s L_r$
R_s, R_r	resistance of stator and rotor coils per phase
J	rotor inertia
B	coefficient of friction
P_p	number of pole pairs
θ_r	rotor electrical angle
ω_s	stator electrical frequency
ω_r	rotor electrical frequency
ω_m	rotor mechanical frequency
ω_m	slip frequency
m_a	modulation index
m_f	frequency ratio (carrier to reference)
C_e	electromagnetic torque

REFERENCES

- [1] A.Nebae, "A new Neutral-Point Clamped PWM Inverter", IEEE Transactions on Industry Applications, Vol.IA-17, N°5, Sept/Oct 1981, pp 518-523.
- [2] P.M.Bhagwat and V.R.Stefanovic, "Generalized Structure of a Multilevel PWM Inverter", IEE, Transactions on Industry Applications, Vol.IA-19, N°6, Nov/Dec 1983, pp 1057-1069.
- [3] Yo- Han Lee, Bum-Seok and Dong-Seo Hyun, A Novel PWM Scheme for three-Level Source Inverter With GTO Thyristors, IEEE Transactions on Industrial Electronics, Vol.32, N°2, Mars/April, 1996.
- [4] P. Rioual, H. Pouliquen, and J.P.Louis, Regulation of a PWM Rectifier in the Unbalanced Network state using Generalized model, IEEE Transactions On Power Electronics, Vol. 11, No 3, pp. 495-499, 1996.
- [5] E. M. Berkouk, Contribution à la conduite des machines asynchrones monophasées et triphasées alimentées par des convertisseurs directs et indirects. Application aux gradateurs et onduleurs multiniveaux. Thèse de doctorat, C.N.A.M, Paris 1996.
- [6] M. Gaad, E. M. Berkouk, K. Aliouane, Contribution à la réalisation de la commande d'un bras d'onduleur à trois niveaux, 2^{ème} conf. intern sur l'électrotechnique, Oran 2000.
- [7] H. Denoun, contribution à l'étude des convertisseurs AC/DC à MLI à facteur de puissance unitaire, application à la conduite de la machine asynchrone. Thèse de Magistère, E.M.P 2001, Alger.
- [8] F. Bouchafaa, E.M.Berkouk and M.S.Boucherit, Analysis and simulation for nine-Level voltage source inverters application to the speed control of the PMSM, Elmelectromotion, Vol.10 N°3 July - September 2003 pp.246-251.

- [9] H. Denoun, N.Benamrouche, S. haddad, S. Meziani and S. Ait Mamar, "A DSP (TMS320lf2407) Based Implementation of PWM for Single-phase AC-DC Bipolar Converter with a Unity Power Factor", WSEAS International Journal of Circuits, Systems and Signal Processing, Vol 5, 2011, pp 354-361 ISSN-1998-4464
- [10] H. Denoun, N.Benamrouche, S. haddad, S. Meziani and S. Ait Mamar, "A DSP (TMS320lf2407) Based Implementation of PWM for Single-phase AC-DC Bipolar Converter with a Unity Power Factor", WSEAS Proceeding of the 10th International Conference on signal Processing, Cobridge, UK February 20-22, 2011, pp-289-295, ISSN 1792-8192.
- [11] C. Panoiu, Baci, M.Panoiu, and C.Cuntan, "Simulation results on the currents harmonics mitigation on the railway station line feed using a data acquisition system" WSEAS Trans. On Electronics, Vol.4, No.11, pp.228-236, 2007.
- [12] H.Tatizawa, E. S. Netsuo, "Calibration of high voltage transducers for power quality measurements," WSEAS Trans. On systems, Vol.8, No, 3, pp.400-409. 2009.
- [13] I.Ghadbane, M. T. Benchouia, "Feed back linearised control based three Phase shunt active power filter," WSEAS Trans. On systems, Vol.7, issue 1, pp.18-25. 2013.



H. Denoun was born in Algiers, Algeria. He received the degree in electrical engineering from the Mouloud Mammeri University, Tizi-Ouzou, Algeria, and the D.E.A degree from Paris6, and the Magister degree from Polytechnic School, Algiers, Algeria in 1998 and 2001 respectively, and his PhD in Electrical Engineering from The

University of Mouloud Mammeri University, Tizi-Ouzou, Algeria.

He is currently a senior lecturer at the same university. His research interests include electrical machines and drives, power electronics and control systems.